Fourier Transform Infrared Evidence of Proton Uptake by Glutamate L212 upon Reduction of the Secondary Quinone Q_B in the Photosynthetic Reaction Center from *Rhodobacter capsulatus*[†]

Eliane Nabedryk,*[,‡] Jacques Breton,[‡] Hemalata M. Joshi,[§] and Deborah K. Hanson[§]

Section de Bioénergétique, Département de Biologie Cellulaire et Moléculaire, CEA/Saclay, 91191 Gif-sur-Yvette Cedex, France, and Biosciences Division, Argonne National Laboratory, 9700 South Cass Avenue, Argonne, Illinois 60439

Received June 16, 2000; Revised Manuscript Received September 6, 2000

ABSTRACT: The photoreduction of the secondary quinone Q_B in native reaction centers (RCs) of *Rhodobacter capsulatus* and in RCs from the GluL212 → Gln and GluL212 → Ala mutants has been investigated at pH 7 in ^1H_2O and ^2H_2O by light-induced Fourier transform infrared (FTIR) difference spectroscopy. The Q_B^-/Q_B FTIR difference spectra reflect changes of quinone−protein interactions and of protonation state of carboxylic acid groups as well as reorganization of the protein upon electron transfer. Comparison of Q_B^-/Q_B spectra of native and mutant RCs indicates that the interactions between Q_B or Q_B^- and the protein are similar in all RCs. A differential signal at ∼1650/1640 cm^{-1}, which is common to all the spectra, is associated with a movement of a peptide carbonyl or a side chain following Q_B reduction. On the other hand, Q_B^-/Q_B spectra of native and mutant RCs display several differences, notably between 1700 and 1650 cm^{-1} (amide I and side chains), between 1570 and 1530 cm^{-1} (amide II), and at 1728−1730 cm^{-1} (protonated carboxylic acid groups). In particular, the latter region in native RCs is characterized by a main positive band at 1728 cm^{-1} and a negative signal at 1739 cm^{-1}. In the L212 mutants, the amplitude of the positive band is strongly decreased leading to a differential signal at 1739/1730 cm^{-1} that is insensitive to $^1H/^2H$ isotopic exchange. In native RCs, only the 1728 cm^{-1} band is affected in ^2H_2O while the 1739 cm^{-1} signal is not. The effects of the mutations and of $^1H/^2H$ exchange on the Q_B^-/Q_B spectra concur in the attribution of the 1728 cm^{-1} band in native RCs to (partial) proton uptake by GluL212 upon the first electron transfer to Q_B, as previously observed in *Rhodobacter sphaeroides* RCs [Nabedryk, E., Breton, J., Hienerwadel, R., Fogel, C., Mäntele, W., Paddock, M. L., and Okamura, M. Y. (1995) *Biochemistry 34*, 14722−14732]. More generally, strong homologies of the Q_B to Q_B^- transition in the RCs from *Rb. sphaeroides* and *Rb. capsulatus* are detected by differential FTIR spectroscopy. The FTIR data are discussed in relation with the results from global proton uptake measurements and electrogenic events concomitant with the reduction of Q_B and with a model of the Q_B turnover in *Rb. sphaeroides* RCs [Mulkidjanian, A. Y. (1999) *FEBS Lett. 463*, 199−204].

In the photosynthetic bacterial reaction center (RC),[1] light-induced electron-transfer reactions lead to a two-electron reduction of the secondary quinone electron acceptor (Q_B) coupled to a two-proton uptake, resulting in the formation of the quinol Q_BH_2, which then dissociates from the RC (*1*). In contrast, the primary quinone acceptor Q_A functions as a one-electron acceptor. In RCs from *Rhodobacter capsulatus* and *Rhodobacter sphaeroides*, Q_A and Q_B are both ubiquinone 10. Although the first electron transfer to Q_A or Q_B in isolated RCs does not involve the direct protonation of the semiquinone itself,[2] substoichiometric proton uptake by the protein following formation of Q_A^- or Q_B^- has been experimentally measured (*3*−*5*) and also predicted from electrostatic calculations (*6*−*11*) based on the X-ray structures. High-resolution structures of the RCs from two purple bacteria, *Rb. sphaeroides* (*12*−*14*) and *Rhodopseudomonas viridis* (*15*−*17*), show that, unlike Q_A, Q_B is surrounded by many ionizable amino acid side chains of the L, M, and H protein subunits. Notably, clusters of electrostatically interacting ionizable residues near Q_B have been identified in the X-ray structures (*16, 18*) and taken into account in electrostatic calculations. Such protonable amino acid residues together with several identified bound internal water molecules (*14, 16*−*20*) can form hydrogen-bonded networks that might be used for the transfer of the protons to the reduced Q_B. Studies of genetically modified RCs from *Rb. sphaeroi-*

[†] This work was in part supported by the U.S. Department of Energy, Office of Biological and Environmental Research, under Contract W-31-109-ENG-38.

* Corresponding author: SBE/DBCM, Bât. 532, CEA/Saclay, 91191 Gif-sur-Yvette Cedex, France. Phone 331 69 08 71 12; fax 331 69 08 87 17; e-mail nabedryk@dsvidf.cea.fr.

[‡] CEA/Saclay.

[§] Argonne National Laboratory.

[1] Abbreviations: FTIR, Fourier transform infrared; RC, reaction center; Q_B/Q_A, secondary/primary quinone.

[2] In chromatophores of *Rb. capsulatus*, a direct protonation of Q_B^- at pH 5 has been reported (*2*).

10.1021/bi0013795 CCC: $19.00
Published on Web 10/28/2000

des and *Rb. capsulatus* have shown that a few amino acids (e.g., SerL223, AspL213, GluL212) are important for rapid coupled electron/proton transfer to Q_B (*21*−*23*). In *Rb. sphaeroides* RCs, the mutation of SerL223 → Ala or Asn greatly reduces the proton-coupled electron-transfer rate (*24*, *25*) while the AspL213 → Asn mutation almost completely blocks transfer of the first proton to reduced Q_B (*26*−*28*). In *Rb. capsulatus* RCs, electron and proton transfer kinetics are drastically decreased in the GluL212-AspL213 → Ala-Ala double mutant compared to native RCs (*29*, *30*). In both RCs, the GluL212 → Gln mutation prevents rapid delivery of the second proton to reduced Q_B (*28*, *31*−*35*). In contrast, the GluL212 → Ala single mutant in *Rb. capsulatus* is photosynthetically competent and retains a fast proton-coupled electron-transfer rate (*33*, *34*, *36*). It shows kinetic rate constants of second electron transfer and of proton uptake only slightly slower, by a factor of 2−3, than those of native RCs. It is worth noting that in RCs from both species, several second-site mutations that compensate for the loss of AspL213 and/or GluL212 have been identified in photocompetent phenotypic revertant strains, suggesting that other residues can substitute for AspL213 or GluL212 to restore proton transfer (*29*, *30*, *33*, *34*, *36*−*41*).

A number of experimental measurements and theoretical calculations have been conducted and are still actively employed to identify which amino acid side chains near Q_B could be proton donors/acceptors. Both native and mutant RCs from *Rb. sphaeroides* and *Rb. capsulatus* are extensively used to investigate the problem of proton uptake upon Q_B reduction. Studies of the pH dependence of proton binding in the Q_B^- state have been interpreted in terms of a group or a cluster with a high pK_a value of about 10.1−10.6 for *Rb. capsulatus* RCs (*23*, *42*) and 9.5 for *Rb. sphaeroides* RCs (*4*, *28*, *31*). This group was associated with GluL212, either directly or indirectly, suggesting that GluL212 has an unusual titration behavior due to strong electrostatic interactions with other residues (*22*, *43*). Measurements of the pH dependence of proton uptake in mutant RCs from *Rb. capsulatus* lacking GluL212 support the proposal that GluL212 is essentially protonated at neutral pH (*34*). Moreover, light-induced photovoltage changes upon formation of Q_B^- measured in wild-type RCs of *Rb. sphaeroides* (*43*) show that the pH dependence of the amplitude of the electrogenic phase follows approximately the measured proton uptake from solution (*4*). In the GluL212 → Gln RCs, the high-pH peak was absent; thus the peak around pH 9.7 in the wild-type RCs was ascribed to proton uptake predominantly by GluL212. All these data have led to the idea that GluL212 contributes to proton uptake only at high pH and is essentially protonated at pH 7. From electrostatic calculations based on the X-ray structures of the *Rb. sphaeroides* RC, it was first proposed that GluL212 is fully (*6*) or partially (*7*) ionized over the whole pH range when Q_B is neutral, becoming protonated following Q_B reduction. The latest calculations by Alexov and Gunner (*10*) indicate that GluL212—which is considered to be part of a cluster of interacting residues that also includes AspL210, AspL213, and SerL223—is protonated at physiological pH in the Q_B state. This cluster of residues is calculated to have a single negative charge (on AspL213) in the ground state (*10*). Furthermore, molecular dynamics simulations of Q_B binding in native *Rb. sphaeroides* RCs also suggest changes of the GluL212/AspL213 protonation states before electron transfer. Both residues would be protonated in the Q_B^- state, while in the neutral Q_B state these calculations are most consistent with either both residues being ionized or GluL212 being protonated and AspL213 being ionized (*44*). On the other hand, kinetic studies from the RCs of the AspL213 → Asn mutant have suggested that AspL213 is ionized in both the Q_B and Q_B^- states (*26*−*28*), thus providing a negative charge stabilizing a proton on or near Q_B.

A direct experimental method for probing changes of the protonation states and/or the environments of Asp and Glu side chains is provided by FTIR difference spectroscopy with trigger-induced reactions (*45*). Bands arising from the carbonyl stretching appear in the region between 1770 and 1700 cm^{-1} (*46*). By use of light-induced FTIR difference spectroscopy, a positive band at 1728 cm^{-1} in the Q_B^-/Q_B spectrum of native RCs from *Rb. sphaeroides* was assigned to substoichiometric proton uptake by GluL212 upon Q_B^- formation, on the basis of its absence when GluL212 was replaced with Gln (*47*, *48*) or Asp (*49*) and its presence in mutants constructed at different sites of the carboxylic acid cluster near Q_B, e.g., at AspL213 and AspL210 (*47*, *50*), or at GluH173 (*51*). $^1H/^2H$ exchange induced a downshift of the frequency of the band at 1728 cm^{-1}, as expected for a protonated carboxylic acid group accessible to solvent. Thus, GluL212 in *Rb. sphaeroides* RCs is partially ionized at pH 7 in the Q_B state becoming protonated in the Q_B^- state. Furthermore, it was concluded that AspL213 and GluH173 do not change protonation state upon Q_B^- formation in native RCs at pH 7 and are mostly ionized in both the Q_B and Q_B^- states (*47*, *51*).

A large number of kinetic electron transfer and proton uptake measurements have been performed on native, mutant, and phenotypic revertant RCs from *Rb. capsulatus* (*23*, *29*, *30*, *33*−*38*, *41*). On the basis of the conservation of the residues around Q_B between RCs from *Rb. capsulatus* and *Rb. sphaeroides* [i.e., sequence identity is greater than 90% (*52*−*54*)], the structure of the Q_B binding site of *Rb. capsulatus* is expected to resemble that of *Rb. sphaeroides* (*55*). As described above, kinetics studies in the RCs of the two species also suggest the similar functional involvement of specific amino acid residues in the coupled electron/proton transfer reactions. It is thus important to directly compare at a submolecular level the changes of protonation state of Asp and Glu residues in the RCs of the two species. In this work, we have used light-induced FTIR difference spectroscopy to perform this comparison. In addition to monitoring changes in the protonation states of carboxylic acid residues, FTIR difference spectroscopy can also detect very small modifications in the protein conformation and the protein−quinone interactions. We have investigated the photoreduction of Q_B in the native RC from *Rb. capsulatus* and in RCs of the GluL212 → Gln and GluL212 → Ala mutants. Light-induced FTIR absorption changes associated with the Q_B to Q_B^- transition have been characterized at pH 7 in ^1H_2O and ^2H_2O. The data are compared to those previously obtained with *Rb. sphaeroides* RCs (*47*, *51*) in order to detect possible homologies concerning proton uptake by Asp/Glu side chains, protein conformation changes, and protein−quinone interactions. A brief account of part of this work has been presented (*56*).

EXPERIMENTAL PROCEDURES

The construction of the GluL212 → Gln mutant and the characterization of the GluL212 → Ala mutant strain have been described (*30, 34, 57*). The AlaL212 mutant was selected as a photocompetent phenotypic revertant of the photosynthetically incompetent AlaL212-AlaL213 double mutant (*30*). Native and mutant RCs were engineered to contain a polyhistidine tag at the C-terminus of the M subunit. This polyhistidine tag has been shown to have no effect on spectroscopic properties of the RC (P. D. Laible, D. Gosztola, D. Holten, C. Kirmaier, M. Schiffer, P. Sebban, A. Taly, M. C. Thurnauer, and D. K. Hanson, unpublished observations) but RC isolation and purification on a Ni^{2+}-affinity column chromatography was greatly simplified. RCs from *Rb. capsulatus* were isolated in 10 mM Tris-HCl, pH 7.8, 0.05% lauryldimethylamine *N*-oxide, and 40 mM imidazole by a procedure modified from that of Goldsmith and Boxer (*58*). After concentration of RCs (0.2−0.5 mM) and elimination of imidazole, the RC samples for FTIR experiments were prepared essentially as reported previously (*47, 51, 59*): to 10 μL of an RC sample (∼0.2 mM) containing an excess of ubiquinone 6 were added 10 μL of ascorbate (10 mM) and diaminodurene (2,3,5,6-tetramethyl-*p*-phenylenediamine; 20 mM) in Tris-HCl (90 mM), pH 7. The solution was dried under argon to a thin paste on a CaF_2 window. The RC sample was then covered with 2 μL of ^1H_2O and sealed with another CaF_2 window. For $^1H/^2H$ isotopic exchange, the RC sample containing the mediators in ^2H_2O was resuspended at least three times in ^2H_2O at 20 °C. This procedure leads to the deuteration of about 60−70% of the peptide NH groups, as judged by the decrease of the amplitude of the amide II band at ∼1550 cm^{-1} (60% peptide NH in-plane bending and 40% C−N stretching) with respect to the amide I band at ∼1660 cm^{-1} (80% peptide C═O stretching) in the absorbance spectrum of the IR sample (data not shown). The Q_B^- state was generated by excitation with a single saturating flash (Nd:YAG laser, 7 ns, 530 nm). Light-induced FTIR difference spectra were recorded at 15 °C with a Nicolet 60SX spectrometer, as described in refs *47* and *59*. Q_A^-/Q_A FTIR difference spectra of the AlaL212 mutant RCs were obtained at pH 7 and at 15 °C in the presence of diaminodurene (20 mM), ascorbate (10 mM), and stigmatellin (2mM) under steady-state continuous illumination as previously reported for *Rb. sphaeroides* RCs (*60, 61*).

RESULTS

Q_B^-/Q_B Spectra of Native and GluL212 → Gln RCs in ^1H_2O. Figure 1a shows the Q_B^-/Q_B light-induced FTIR difference spectrum of native RCs from *Rb. capsulatus* in ^1H_2O. The corresponding spectrum for the GlnL212 mutant RC is displayed in Figure 2a. In such difference spectra, negative bands originate from the neutral Q_B state and positive bands arise from the Q_B^- state. The Q_B^-/Q_B spectra of wild-type and GlnL212 RCs display typical absorption changes associated with Q_B reduction (*47, 62, 63*). In both spectra, several common major peaks are observed, at ∼1650 and 1480 cm^{-1} for the positive bands and at 1739, 1659, 1640, 1615−1613, ∼1290, and 1265 cm^{-1} for the negative bands. Moreover, the spectra of *Rb. capsulatus* RCs present a large number of features common to those of *Rb. sphaeroides* RCs (*47, 62, 63*). On the basis of studies of *Rb. sphaeroides* RCs reconstituted with isotope-labeled ubiquinones (*63, 64*) and of comparison with redox-induced anion difference spectra of ubiquinone in solution (*65, 66*), assignments of the neutral and anion quinone modes in the Q_B^-/Q_B spectrum have been established. The 1479−1480 cm^{-1} peak in the Q_B^-/Q_B spectra of *Rb. capsulatus* RCs (Figures 1a and 2a) can be similarly assigned to the semiquinone (C···O and C···C) modes. The 1640 and 1615−1613 cm^{-1} bands correspond to the bands observed at 1640−1642 and 1617−1614 cm^{-1} in *Rb. sphaeroides* RCs, which

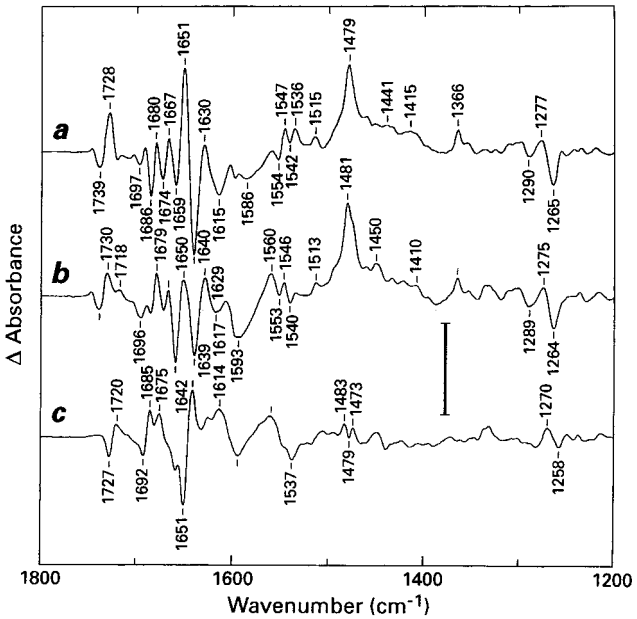

FIGURE 1: Light-induced Q_B^-/Q_B FTIR spectra of wild-type reaction centers of *Rb. capsulatus* at pH 7 and at 15 °C with single-turnover flash excitation. (a) ^1H_2O; (b) ^2H_2O; (c) ^2H_2O minus ^1H_2O double-difference spectrum. About 60 000 scans were averaged. Spectral resolution was 4 cm^{-1}. The bar represents 5×10^{-4} absorbance units. The position of the bands is given at ±1 cm^{-1}.

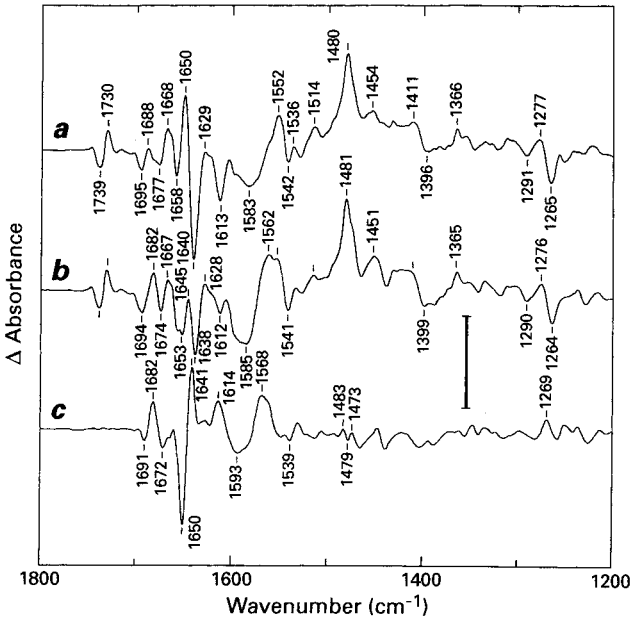

FIGURE 2: Light-induced Q_B^-/Q_B FTIR spectra of the GluL212 → Gln mutant RCs of *Rb. capsulatus* at pH 7 and at 15 °C with single-turnover flash excitation. (a) ^1H_2O; (b) ^2H_2O; (c) ^2H_2O minus ^1H_2O double-difference spectrum. Same conditions as in Figure 1.

arise at least partly from the C═O and the C═C modes of Q_B, respectively. Similarly, contributions from the methoxy groups of Q_B are also present at ~1290 and 1265 cm^{-1} in spectra of *Rb. capsulatus* RCs. The two latter bands together with the semiquinone positive band at 1479−1480 cm^{-1} were used to normalize Q_B^-/Q_B spectra of native and mutant RCs by minimizing the net difference between two spectra in these regions (*47, 51*). Variations by ±10% of the optimum coefficient selected from the interactive subtraction do not lead to a significant perturbation of the double-difference spectra (data not shown).

The resemblance of the quinone and semiquinone modes described above in the Q_B^-/Q_B spectra of wild-type and GlnL212 mutant RCs from *Rb. capsulatus* therefore indicates that the interactions between Q_B or Q_B^- and the protein are similar in these two RCs. Moreover, such interactions appear to be homologous to the ones observed in *Rb. sphaeroides* RCs (*47, 63, 64*). Several protein (backbone and/or side chains) signals are also common to Q_B^-/Q_B spectra of wild-type (Figure 1a) and GlnL212 mutant (Figure 2a) *Rb. capsulatus* RCs, i.e., the large differential signal at 1651−1650/1640 cm^{-1} (mainly amide I, although both quinone and peptide carbonyls are expected to contribute at 1640 cm^{-1}) and the bands at 1668−1667 cm^{-1} (+) and 1659−1658 (−) cm^{-1}. Some differences are, however, observed between Q_B^-/Q_B spectra of native and GlnL212 RCs of *Rb. capsulatus*, i.e., between 1700 and 1670 cm^{-1} (backbone and/or side chains), between 1570 and 1530 cm^{-1} (amide II), and at 1728−1730 cm^{-1}. For example, in the amide II region, a small signal is observed at 1547 (+) cm^{-1} in the Q_B^-/Q_B spectrum of wild-type *Rb. capsulatus* RCs (Figure 1a), in contrast to the broad positive band peaking at 1552 cm^{-1} in the spectrum of the GlnL212 mutant (Figure 2a). In the Q_B^-/Q_B spectra of *Rb. sphaeroides* RCs, the main amide II signal was observed at 1537 (+) cm^{-1} but had a different shape in the wild type and the GlnL212 mutant (*47*). With respect to *Rb. sphaeroides* RCs, additional negative bands are seen in the spectrum of wild-type *Rb. capsulatus* RCs at 1674 and 1659 cm^{-1}. It is clear that the ~1650/1640 cm^{-1} differential signal is common to all spectra. In both *Rb. capsulatus* (Figure 1a) and *Rb. sphaeroides* RCs, a pronounced negative band at 1686−1685 cm^{-1} is present in native RCs but it is absent in RCs of the GluL212 → Gln mutant (*47*; Figure 2a).

In the region between 1770 and 1700 cm^{-1}, signals arising from the C═O stretching mode of protonated Asp and Glu residues are expected to give absorption changes. In addition, 10a-ester C═O modes of the intermediary electron acceptor H_A or of the bacteriopheophytin H_B can also contribute (*61, 67*). The Q_B^-/Q_B spectrum of wild-type *Rb. capsulatus* RCs displays a main positive band at 1728 cm^{-1} and a negative signal at 1739 cm^{-1} (Figure 1a). These peaks were also observed in the spectrum of *Rb. sphaeroides* RCs with, however, a much lower amplitude of the negative signal at 1740 cm^{-1} (*47, 51*). In the GlnL212 mutant RC (Figure 2a), the amplitude of the positive signal is strongly decreased, leading to a differential signal positive at 1730 cm^{-1} and negative at 1739 cm^{-1}. Note that a differential signal was observed at 1740/1732 cm^{-1} in the corresponding mutant of *Rb. sphaeroides* (*47*), but its amplitude was several times smaller than in the *Rb. capsulatus* GlnL212 mutant. COO^- stretching modes of carboxylate groups could contribute to the broad negative signals at around 1586−1583 cm^{-1} (antisymmetric) and 1390 cm^{-1} (symmetric) (Figures 1a and 2a). A small negative band at 1709 cm^{-1} has been previously observed in the Q_B^-/Q_B spectrum of wild-type *Rb. capsulatus* RCs (*59*). This signal is not seen in Figure 1a. RCs used in ref *59* were isolated by standard procedures and it was noticed that the amplitude of the absorption changes associated with the photoreduction of Q_B was low, i.e., about 4−5-fold smaller in *Rb. capsulatus* than in *Rb. sphaeroides* when the RC samples are normalized to the amide I absorption. Here, with polyhistidine-tagged RCs, the amplitude of the absorption changes in Figure 1a is about 5-fold larger than in our previous work (*59*) The few differences that can be seen between the two sets of data obtained in ref *59* and shown in Figure 1 are most probably due to the improved quality of the RCs used in the present study.

(2) Q_B^-/Q_B Spectra of Native and GluL212 → Gln RCs in ^2H_2O. Figures 1b and 2b show the Q_B^-/Q_B spectra in ^2H_2O of *Rb. capsulatus* RCs from wild type and the GlnL212 mutant, respectively, to identify bands that are sensitive to $^1H/^2H$ isotopic exchange. These spectra also exhibit several features similar to those found in *Rb. sphaeroides* RCs (*47*). Notably, the quinone bands do not shift significantly upon $^1H/^2H$ exchange, and the main anion band of Q_B^- in *Rb. capsulatus* RCs also peaks at 1481 cm^{-1} in ^2H_2O compared to 1479 cm^{-1} in ^1H_2O. The most noticeable changes occur in the spectral region between 1735 and 1640 cm^{-1} and at 1593, 1560−1568, and 1537−1539 cm^{-1}, as previously observed for *Rb. sphaeroides* RCs (*47*). In particular, the amplitude of the main differential signal at ~1650/1640 cm^{-1} is reduced in all the spectra obtained in ^2H_2O. All these changes are best seen in the Q_B^-/Q_B double-difference spectra shown in Figures 1c and 2c, calculated from the Q_B^-/Q_B spectrum obtained in ^2H_2O (Figures 1b and 2b) minus the Q_B^-/Q_B spectrum obtained in ^1H_2O (Figures 1a and 2a). Several corresponding signals appear in the ^2H_2O minus ^1H_2O spectra of the wild type (Figure 1c) and GlnL212 mutant (Figure 2c), notably at ~1650, 1593, and 1537−1539 cm^{-1} for the main negative bands and at 1682−1685, ~1641, 1614, and 1560−1568 cm^{-1} for the positive bands.

In the C═O stretching region of protonated carboxylic groups, a main change occurs in native RCs in ^2H_2O as indicated by the drop in intensity of the positive band at 1728 cm^{-1} and the appearance of a new positive peak at 1718 cm^{-1} (Figure 1b). The negative signal at 1739 cm^{-1} is not affected in ^2H_2O, suggesting that it does not arise from a carboxyl group. These changes are best seen in Figure 1c, where a negative band at 1727 cm^{-1} and a positive band at ~1720 cm^{-1} reflect the frequency downshift of a protonated carboxylic group from ^1H_2O to ^2H_2O. In contrast, the region between 1770 and 1700 cm^{-1} is completely flat in the double-difference spectrum (^2H_2O minus ^1H_2O) of the GluL212 → Gln mutant (Figure 2c), reflecting the insensitivity to $^1H/^2H$ exchange (Figure 2b) of the 1739/1730 cm^{-1} differential signal observed in the direct Q_B^-/Q_B spectrum of GlnL212 RCs (Figure 2a). Thus, the 1739/1730 cm^{-1} differential signal cannot be assigned to a shift of a protonated carboxylic group in the GlnL212 mutant RCs. The absence of a significant $^1H/^2H$ exchange effect in the carboxylic acid region has been also observed in the GluL212 → Gln mutant of *Rb. sphaeroides* (*47*). From all the present IR data, it can be concluded that, similarly to *Rb. sphaeroides*, no change of

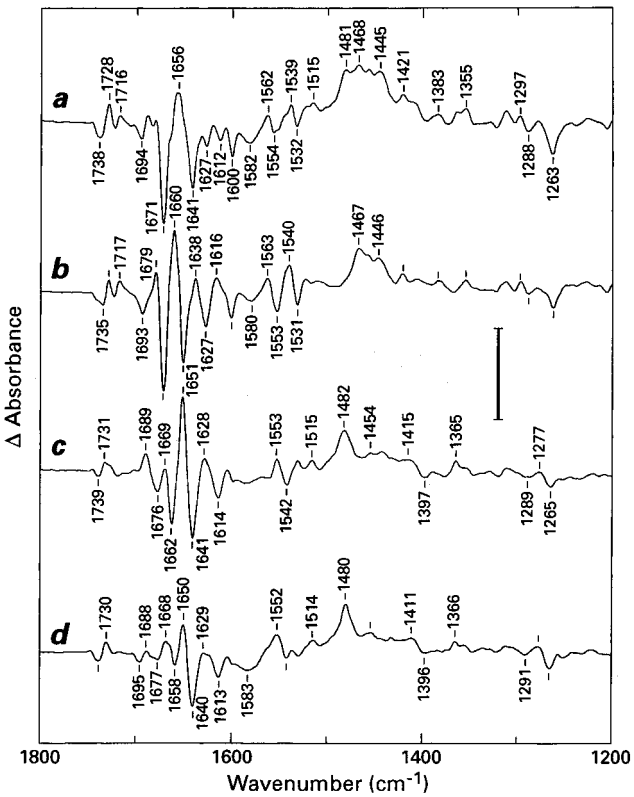

FIGURE 3: Light-induced FTIR difference spectra of the GluL212 → Ala mutant RCs of *Rb. capsulatus* at pH 7 and at 15 °C in ^1H_2O under steady-state continuous illumination. (a) Light-induced FTIR difference spectrum containing both Q_A^-/Q_A and Q_B^-/Q_B contributions. (b) Q_A^-/Q_A FTIR difference spectrum. (c) Calculated Q_B^-/Q_B FTIR difference spectrum obtained by subtracting the Q_A^-/Q_A spectrum displayed in panel b from the light-induced spectrum shown in panel a. (d) Q_B^-/Q_B FTIR difference spectrum of GluL212 → Gln RCs of *Rb. capsulatus*. The bar represents 10^{-3} absorbance units.

protonation state of carboxylic acid groups occurs upon Q_B reduction in GlnL212 mutant *Rb. capsulatus* RCs, in contrast to native RCs (Figure 1a), where the 1728 cm^{-1} peak reflects the (partial) protonation of GluL212.

(3) Q_B^-/Q_B Spectrum of GluL212 → Ala RCs in ^1H_2O. Several attempts were made to generate a pure Q_B^-/Q_B spectrum of the GluL212 → Ala mutant under the usual conditions previously described (*47*, *59*, *63*, *64*). Despite varying several parameters (concentrations of reactants, detergent concentration, changing the pH from 7 to 5), we could not selectively photoreduce Q_B in this mutant. The light-induced FTIR difference spectrum of an IR sample of AlaL212 *Rb. capsulatus* RCs (in the presence of mediator and reductant, as described under Experimental Procedures) shown in Figure 3a was obtained either by flash excitation or under steady-state continuous illumination. In this spectrum, the negative bands at 1641 and 1612 cm^{-1} and the positive one at 1481 cm^{-1} are probably due to the Q_B to Q_B^- transition. On the other hand, several signals are highly reminiscent of Q_A^-/Q_A bands of *Rb. sphaeroides* RCs, notably the pronounced negative band at 1671 cm^{-1}, the one at 1600 cm^{-1}, and the positive band at 1468 cm^{-1} (*60*, *61*). Note that Figure 3a does not show any contributions arising from the oxidation of the primary electron donor (*68*) or the photoreduction of H_A (*69*). It must also be emphasized that all the bands of the composite light-induced spectrum (Figure 3a) decay at the same rate (tens of seconds).

The Q_A to Q_A^- transition was therefore investigated in the AlaL212 mutant in the presence of stigmatellin to block the Q_A to Q_B electron-transfer reaction. The Q_A^-/Q_A light-induced FTIR difference spectrum of AlaL212 mutant RCs is displayed in Figure 3b. This spectrum compares fairly well with the Q_A^-/Q_A spectrum previously obtained from *Rb. sphaeroides* RCs (*60*, *61*). Most of the features observed in wild-type *Rb. sphaeroides* RCs and assigned to specific modes are found in Figure 3b. By use of *Rb. sphaeroides* RCs reconstituted with site-specific isotopically labeled ubiquinones (*70*−*72*), the C_1═O and C_4═O modes of Q_A were localized at 1660 and 1601 cm^{-1}, respectively, and the C═C mode of Q_A at 1628 cm^{-1}. The main C···O anion band of Q_A^- was found at 1466 cm^{-1}, with shoulders at 1484 and 1420 cm^{-1} assigned to C···C modes. In the Q_A^-/Q_A spectrum of AlaL212 mutant *Rb. capsulatus* RCs (Figure 3b), corresponding bands are directly observed at 1627 (−), 1600 (−), 1467 (+), and 1421(+) cm^{-1} and are assigned to C═C (Q_A), C═O (Q_A), C···O (Q_A^-), and C···C (Q_A^-) modes, respectively. In addition, a number of protein bands (backbone and side chains) are also very close in both spectra, i.e., at 1671 (−), 1563 (+), 1553 (−), 1540 (+), and 1531 (−) cm^{-1}, as well as peaks at 1735 (−), 1728 (+), 1717 (+), 1693 (−), 1660 (+), 1383 (+), 1355 (+), 1297 (+), and 1263 (−) cm^{-1}.

Comparison of spectra a and b in Figure 3 shows that spectrum a displays a number of signals due to the Q_A to Q_A^- transition, e.g., the main ones are seen at 1671 (−), 1627 (−), 1600 (−), 1562 (+), 1554 (−), 1539 (+), 1532 (−), 1468 (+), and 1421 (+) cm^{-1}. On the other hand, the negative bands at 1641 and 1612 cm^{-1} are typical of the Q_B to Q_B^- transition. It therefore appears that the light minus dark FTIR spectrum obtained for the AlaL212 mutant RCs (Figure 3a) is a mixture of Q_B^-, Q_B, Q_A^-, and Q_A signals. The Q_B^-/Q_B spectrum of AlaL212 RCs (Figure 3c) was calculated by subtracting the Q_A^-/Q_A spectrum (Figure 3b) from the spectrum shown in Figure 3a; the net difference at 1671 cm^{-1} was minimized, which also results in the minimization of the 1600 cm^{-1} band. For the ease of comparison, the spectrum of GlnL212 RCs is also displayed in Figure 3d. Similarly to GlnL212 mutant RCs, the C═O and C═C modes of Q_B in RCs of the AlaL212 mutant are observed at 1641 and 1614 cm^{-1}, respectively, and the main semiquinone mode peaks at 1482 cm^{-1} (Figure 3c). Comparison of the two mutant spectra shows additional similar features at ∼1650/1640 cm^{-1}, 1688−1689 (+), 1676−1677 (−) cm^{-1}, 1553/1542 cm^{-1}, 1515−1514 cm^{-1}, and between 1460 and 1200 cm^{-1}. However, the amplitude of the differential signal at 1651/1641 cm^{-1} and of the bands at 1689 (+), 1676 (−), 1669 (+), and 1662 (−) cm^{-1} (this latter band is probably equivalent to the 1658 cm^{-1} band of the GlnL212 mutant) is significantly larger in the calculated Q_B^-/Q_B spectrum of the AlaL212 RCs than in the direct experimental spectrum obtained for GlnL212 RCs. Although it cannot be excluded that a small part of these differences can be due to the procedure of interactive subtraction used to calculate the Q_B^-/Q_B spectrum of the AlaL212 mutant RCs, these observations more probably reflect larger changes of peptide backbone and/or side-chain groups in the AlaL212 RCs than in the GlnL212 RCs.

Furthermore, the Q_B^-/Q_B spectrum of AlaL212 mutant RCs (Figure 3c) also shows a negative signal at 1739 cm^{-1} and a positive one at 1731 cm^{-1}, as observed for the GlnL212

mutant (Figure 3d). Although the band at 1731 cm^{-1} appears broader in RCs of AlaL212 than in those of the GlnL212 mutant, the large positive peak seen at 1728 cm^{-1} in native RCs is also absent in AlaL212 RCs. Thus, the data obtained for the AlaL212 mutant corroborate those obtained for the GlnL212 mutant RCs and strengthen the attribution of the positive band at 1728 cm^{-1} in native RCs to proton uptake by GluL212 upon Q_B reduction.

DISCUSSION

In this work, we have performed light-induced FTIR studies of native *Rb. capsulatus* RCs and mutant RCs (site-directed or spontaneous) in which GluL212 was replaced with Gln or Ala (*30*). In *Rb. sphaeroides* RCs, it has been shown previously that substoichiometric proton uptake by GluL212 occurs upon photoreduction of Q_B (*47, 48, 50, 51*). Here, we report a similar situation in *Rb. capsulatus* RCs. We start with a comparison of Q_B^-/Q_B spectra of *Rb. capsulatus* and *Rb. sphaeroides* RCs. We then discuss the protonation of GluL212 in response to the formation of Q_B^- in *Rb. capsulatus* RCs. We end with a comparison of FTIR data with several spectroscopic studies of Q_B reduction (electron-transfer kinetics, proton uptake measurements and electrogenic events) and a discussion in relation with a mechanistic model of the Q_B turnover in *Rb. sphaeroides* RCs recently proposed by Mulkidjanian and co-workers (*73*−*75*).

(1) Strong Homologies of the Q_B to Q_B^- Transition in Rb. capsulatus and Rb. sphaeroides RCs As Detected by Differential FTIR. The Q_B binding pocket of *Rb. sphaeroides* is taken as a model for that of *Rb. capsulatus* on the basis of the conservation of most of the residues surrounding Q_B in both RCs (*55*). In *Rb. sphaeroides*, the side chains of HisL190, SerL223, IleL224 (Val in *Rb. capsulatus*), and GlyL225 are in proximity to the carbonyls of Q_B (at least in the proximal position of the quinone seen in ref *19)*, and a cluster of interacting acidic and basic residues located near Q_B has been described (*18*). Such a cluster probably also exists in the *Rb. capsulatus* RC, since identical residues are found at the same positions, i.e., GluL212, AspL213, AspL210, and ArgL217, and at homologous positions, i.e., GluH175, AspH127, LysH133, and ArgH179 (GluH173, AspH124, LysH130 and ArgH177 in *Rb. sphaeroides*, respectively) (*52*−*54*). The only change is the replacement of AspM17 in the *Rb. sphaeroides* RC by Glu in *Rb. capsulatus*. In *Rb. sphaeroides* RCs, several possible pathways for proton transfer to reduced Q_B have been proposed (*14, 16, 18*−*20*), based on crystallographically observed networks of protonatable amino acids and internal water molecules. These pathways connect SerL223, GluL212, and AspL213 to the external surface.

In *Rb. capsulatus* RCs, a number of potential pathways for proton transfer to Q_B have also been proposed (*29, 30, 36*−*38, 41)*. The existence of multiple pathways was inferred by the spectroscopic demonstration that proton uptake can be restored by distant compensatory mutations in RCs that also carry site-specific mutations that interrupt that process. Since most of the internal (listed above) and connecting residues located near the surface of the protein, i.e., AspM240, TyrM3, and AspM17 (Glu in *Rb. capsulatus*) are conserved (*52*−*54*) in both *Rb. sphaeroides* and *Rb. capsulatus* (except for GluH224, which is changed to ValH226; however, H225 is Asp in *Rb. capsulatus* while it is Thr in *Rb. sphaeroides*), similar proton transfer pathways are likely to exist in both RCs. In *Rb. sphaeroides* RCs, recent studies of the binding of metal ions (which inhibit the rates of reduction and protonation of Q_B) indicate that there is one dominant site of proton entry into the wild-type RC near AspH124, HisH126, and HisH128 (*76, 77*). These three residues are also conserved in the sequence of the H subunit of *Rb. capsulatus* RCs (*53*).

In agreement with the high homology of the residues around Q_B in both RCs, the Q_B^-/Q_B spectra of native and mutant RCs from *Rb. capsulatus* and *Rb. sphaeroides* display a number of common features both in the protein (side chain and backbone) and the quinone/semiquinone absorption regions. Notably, the C═O (at ∼1640 cm^{-1}) and C═C (at ∼1615 cm^{-1}) modes of Q_B and the C⋯O (at ∼1480 cm^{-1}) modes of Q_B^- are very close in the two species. This indicates that the interactions between Q_B or Q_B^- and the surrounding amino acid residues are similar in RCs of *Rb. capsulatus* and *Rb. sphaeroides*. The differential signal at ∼1650/1640 cm^{-1}, which is observed in all native and mutant RCs (Figures 1a, 2a, and 3c; see also ref *47*) is attributed in part to a conformational change or a movement of a backbone C═O or of a side chain following Q_B reduction. The negative signal observed at 1686 cm^{-1} in the Q_B^-/Q_B spectrum of wild-type *Rb. capsulatus* RCs (Figure 1a) can be compared to the one observed at ∼1685 cm^{-1} in the Q_B^-/Q_B spectra of native *Rb. sphaeroides* RCs and of mutants that do not contain the GluL212 → Gln substitution (*47, 50, 51*). This negative signal at 1686 cm^{-1} is observed neither in the GlnL212 (Figure 3d) nor in the AlaL212 (Figure 3c) mutant RCs, suggesting that it is directly or indirectly due to the loss of the glutamic acid residue at position L212. As previously proposed in *Rb. sphaeroides*, the negative band at 1686 cm^{-1} in the Q_B^-/Q_B spectrum of native *Rb. capsulatus* RCs (Figure 1a) is tentatively interpreted in terms of a change of absorption of the peptide C═O of GluL212 that is affected by the photoreduction of Q_B.

Spectral similarities between the RCs of *Rb. capsulatus* and *Rb. sphaeroides* also clearly appear by comparing the double-difference spectra ^2H_2O minus ^1H_2O (Figures 1c and 2c; see also ref *47*). They are even more apparent in the double-difference spectra (native minus mutant), calculated from the Q_B^-/Q_B spectrum obtained for the wild-type RCs minus the Q_B^-/Q_B spectrum obtained for RCs of a GlnL212 mutant of the corresponding species. That double-difference spectrum is shown for *Rb. capsulatus* RCs in Figure 4a between 1750 and 1600 cm^{-1}, together with the equivalent double-difference spectrum from *Rb. sphaeroides* RCs previously reported in ref *47* (Figure 4b). These double-difference spectra appear somewhat simpler than the direct Q_B^-/Q_B spectra, depicting only a few negative and positive bands. In both species (Figure 4), similar positive peaks are found at 1728−1727, 1693−1694, 1679−1677, and 1651 cm^{-1}, while negative peaks appear at 1685 and 1662−1658 cm^{-1}. In addition, a differential signal common to both double-difference spectra is localized in the amide II region at ∼1553/1543 cm^{-1} (data not shown). All these IR data converge to demonstrate that most of the chemical groups affected by the GluL212 → Gln mutation or by $^1H/^2H$ exchange upon formation of Q_B^- are the same in the RCs of the two species.

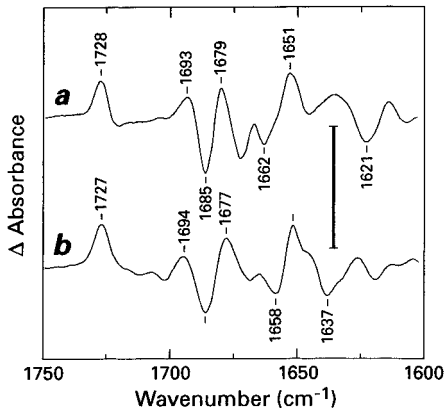

FIGURE 4: Calculated double-difference spectra in the 1750−1600 cm^{-1} region between Q_B^-/Q_B FTIR spectra of the wild-type RCs and the GluL212→Gln mutant (wild-type minus Gln L212 mutant) in ^1H_2O upon normalization on the 1479−1480 cm^{-1} semiquinone anion band. (a) *Rb. capsulatus*; (b) *Rb. sphaeroides* (*47*). The bar represents 5×10^{-4} absorbance units.

A few features are, however, specific to the Q_B^-/Q_B spectra of *Rb. capsulatus* RCs, notably the negative bands at 1658−1659 and 1674−1677 cm^{-1}, which are observed in both wild-type (Figure 1a) and GlnL212 mutant (Figure 2a) RCs. Corresponding signals are seen at 1662 and 1676 cm^{-1} in AlaL212 RCs (Figure 3c). These signals, whose frequencies and amplitudes are affected in ^2H_2O, could reflect additional changes in backbone C═O and/or side chains [such as Asn, Arg, or Gln (*78*)]. The absorption changes in the amide II region are also different in *Rb. capsulatus* and *Rb. sphaeroides* RCs.

A broad continuum band at ∼2600 cm^{-1} in ^1H_2O, shifting to ∼2100 cm^{-1} in ^2H_2O, is observed in the Q_B^-/Q_B spectra of native and GlnL212 mutant RCs of *Rb. capsulatus* (data not shown). This band does not appear to be sensitive to the GlnL212 mutation. Comparable bands have been previously observed in native *Rb. sphaeroides* RCs at identical frequencies as well as in *Rps. viridis* RCs at ∼2800 cm^{-1} in ^1H_2O and at ∼2200 cm^{-1} in ^2H_2O (*79*). These IR continua have been interpreted in terms of highly polarizable hydrogen bonds (*80*) in a large web involving carboxylic acid groups and/or polar residues and ordered water molecules (*79*).

(2) GluL212 Undergoes Protonation in Response to the Formation of Q_B^-. The present FTIR data on the photoreduction of Q_B in *Rb. capsulatus* RCs show that the protonation of a carboxylic acid group occurs at 1728 cm^{-1}. As expected for a carboxylic acid, the band downshifts ∼10 cm^{-1} in ^2H_2O, as seen in Figure 1. Both the frequency and extent of $^1H/^2H$ exchange-induced downshift are almost identical to those in the Q_B^-/Q_B spectrum of *Rb. sphaeroides* RCs (*47*). Moreover, in both RCs, the effect of the GluL212 → Gln mutation results in a decrease of the amplitude of the 1728 cm^{-1} band while the negative signal at 1739−1740 cm^{-1} remains unaffected by the mutation. The result is the observation of a differential signal negative at 1739−1740 cm^{-1} and positive at 1730−1732 cm^{-1} in mutants of GluL212. ^2H_2O does not cause any significant frequency shift or amplitude change of this differential signal. It therefore appears that the effects of the GluL212 → Gln mutation and of $^1H/^2H$ exchange on the Q_B^-/Q_B spectra of *Rb. capsulatus* RCs concur in the assignment of the 1728 cm^{-1} signal in native RCs to proton uptake by GluL212 upon Q_B^- formation, as previously observed for *Rb. sphaeroides* RCs (*47, 51*). Thus, in native RCs at pH 7, GluL212 is also at least partially ionized in the Q_B neutral state and becomes more protonated in the semiquinone state.

The results obtained from the calculated Q_B^-/Q_B spectrum of the AlaL212 mutant of *Rb. capsulatus* are fully consistent with the data obtained on GlnL212 RCs. In the carboxylic region of the Q_B^-/Q_B spectrum of the AlaL212 mutant RC (Figure 3c), the negative (at 1739 cm^{-1}) and positive (at 1731 cm^{-1}) signals are comparable to those seen in the GlnL212 spectrum (Figure 3d). Note that in L212 mutant RCs of *Rb. capsulatus*, the differential signal at 1739/1730−1731 cm^{-1} is severalfold larger than the corresponding small negative signal at 1740/1732 cm^{-1} found in *Rb. sphaeroides* RCs (*47*). The positive signal at ∼1730 cm^{-1} that remains in RCs of L212 mutants thus has to be taken into account (as a background) to calculate the integrated absorption of the positive band at 1728 cm^{-1} in the Q_B^-/Q_B spectrum of native *Rb. capsulatus* RCs. From the present work, it appears that the intensity of the 1728 cm^{-1} band is comparable in native RCs of both *Rb. sphaeroides* and *Rb. capsulatus*, indicating a similar proton uptake (±10%) by GluL212 in the two RCs, which is estimated to be 0.3−0.4 H^+/Q_B^- (*47*).

In the GluL212 → Gln mutant of *Rb. sphaeroides*, we had previously proposed that the small differential at 1740/1732 cm^{-1} might in part involve a shift of the 10a-ester C═O mode of the bacteriopheophytin H_B, due to the presence of an electron on Q_B (*47*). An electrostatic influence of Q_A reduction on the IR mode of the 10a-ester C═O of H_A has been recently demonstrated by studies of mutant RCs of *Rb. sphaeroides* (at sites GluL104 and TrpL100) (*61*) and *Rps. viridis* (at sites GluL104 and TrpM250) (*67, 81*). In *Rps. viridis* RCs, an electrochromic effect on the 10a-ester C═O vibration of H_A has been also detected upon Q_B reduction, although with a smaller amplitude (*81*). In the GlnL212 and AlaL212 mutants of *Rb. capsulatus*, the differential signal at 1739/1730 cm^{-1} could similarly account for the electrostatic influence of Q_B^- on the IR mode of the 10a-ester C═O of H_A and H_B. The same interpretation can be used for the differential signal observed at 1739/1730 cm^{-1} in native RCs in ^2H_2O.

(3) Comparison with Other Spectroscopic Studies.

Effect of Mutations on the $Q_A^-Q_B \leftrightarrow Q_AQ_B^-$ Equilibrium. Kinetic electron-transfer measurements show that the $P^+Q_B^-$ charge recombination rates (k_{BP}) are higher in GlnL212 and AlaL212 mutant RCs than in native RCs, with the greatest rate observed in the AlaL212 RC, i.e., ∼5 s^{-1} at pH 7 compared to ∼0.7 s^{-1} for the wild type (*34*). This suggests a higher energy level for Q_B^- in AlaL212 RCs than in GlnL212 (and wild-type) RCs. According to our measurements, it is not possible to generate a pure Q_B^-/Q_B spectrum in AlaL212 RCs under the conditions that we usually employ to form the Q_B^- state. We always obtained additional contributions from the Q_A^- state. Our observations are thus fully in agreement with kinetic data indicating a lower energy gap between $Q_A^-Q_B$ and $Q_AQ_B^-$ in the AlaL212 RC as compared to the GlnL212 mutant RC (*34*).

Amplitudes of Proton Uptake. Spectroscopic measurements with indicator dyes have determined that a total of 0.7 H^+/Q_B^- are taken up at pH 7.5 by native *Rb. capsulatus* RCs (*5, 34*), while FTIR experiments at pH 7 show uptake of ∼0.3−0.4 H^+ in the carboxyl region (i.e., H^+/Q_B^-/GluL212)

of the spectrum. This difference is not unexpected since the former approach measures total proton uptake by the RC. On the other hand, only proton uptake by carboxylic acid residues and redistribution among such residues in the interior of the RC are directly monitored by differential FTIR in the 1770−1700 cm^{-1} range. Comparison of the two approaches leads us to propose that about half of the total proton uptake measured at pH 7 upon Q_B reduction involves noncarboxylic residues. The continuum band observed at 2600 cm^{-1} in the Q_B^-/Q_B spectrum of native RCs which is thought to reflect proton uptake by a highly polarizable hydrogen-bond network (*79*) could contribute to the differences in the amplitudes of proton uptake observed in wild-type RCs at pH 7−7.5 by the two different techniques.

Measurements of proton uptake upon formation of Q_B^- have been reported for both GlnL212 and AlaL212 mutant RCs of *Rb. capsulatus* (*5, 34*). At pH 7.5, there is no large difference between the RCs of the wild type and the L212 mutants. A total of 0.63 and 0.55 H^+/Q_B^- are taken up by GlnL212 and AlaL212 RCs, respectively, compared to 0.7 H^+/Q_B^- in the wild type (*5*). On the other hand, no proton uptake by carboxylic acid groups is detected by FTIR spectroscopy in the GlnL212 and AlaL212 mutants. A larger difference in the amplitude of proton uptake between wild-type and L212 mutant RCs is thus observed by FTIR (at pH 7), i.e., ∼0.3−0.4 H^+, compared to an average of 0.1 H^+ determined by use of pH indicator dyes (at pH 7.5). Both series of measurements are, however, compatible if we assume that the protonation of Glu L212 in native RCs is compensated in the L212 mutants by proton uptake by one or several noncarboxylic groups with pK_as comparable to that of GluL212 in wild-type RCs. In agreement with this proposal, the larger electrogenic signal observed around pH 7 in the L212Gln mutant compared to wild-type RCs has been interpreted in terms of compensating proton uptake by other titrating residues (*43*).

In the mutant RCs, the loss of GluL212 does not significantly change the amount of proton uptake between pH 7 and 8−8.5, but H^+/Q_B^- drastically decreases at pH 9−10 (*34*). The stoichiometries of proton uptake by the Q_B^- state in wild-type *Rb. capsulatus* RCs (as well as in *Rb. sphaeroides*) show a pH dependence with two distinct maxima at pH ∼6 and ∼10−11 (*4, 23, 34, 42*); these proton uptake data for *Rb. capsulatus* RCs were fitted to five groups with distinct pK_as (*23, 42*). The group with the highest pK_a (10.3−11.6) has been associated with GluL212, either directly or indirectly. Thus, proton uptake measurements as well as electrogenicity measurements support the idea that GluL212 contributes to proton uptake essentially at high pH (*34, 43*). On the other hand, FTIR data on *Rb. capsulatus* and *Rb. sphaeroides* RCs show that GluL212 already contributes to proton uptake at pH 7. Thus, a more complicated model for protonation must be invoked to take into account all these data. Such a model would involve heterogeneity of the protonation state of GluL212 in wild-type RCs with at least two distinct pK_as for GluL212.

(4) The Mulkidjanian Model. Recently, a mechanistic model of the Q_B turnover in *Rb. sphaeroides* RCs has been discussed on the basis of X-ray structures and studies of electrogenic events (*73*−*75*). In chromatophores of *Rb. sphaeroides*, kinetics of the electrogenic reactions of the Q_B to Q_B^- transition clearly show two components at subambient temperature (*73*). To explain this kinetic heterogeneity, Mulkidjanian and co-workers (*73*−*75*) suggested two possible conformational states of the neutral quinone and an equilibrium between two populations of GluL212 (protonated Glu-COOH and ionized Glu-COO^-). One conformational state is stabilized by a hydrogen bond between the COOH of GluL212 and the methoxy oxygen O3 of the Q_B ring [compatible with the X-ray crystal structure from El-Kabbani et al. (*13*)] and the other lacks this bond. In the latter configuration of the quinone, which corresponds to the distal position of Q_B in the X-ray structure (*19;* see also ref *17* for *Rps. viridis*), two water molecules form a bridge between GluL212 (hydrogen-bond acceptor) and HisL190 (hydrogen-bond donor), and thus GluL212 is in its ionized state at neutral pH (*73*−*75*). The former configuration of Q_B would correspond to the proximal position, and the protonated form of GluL212 is stabilized by a hydrogen bond to the quinone. The formation of the hydrogen bond is assumed to be responsible for the high pK_a of GluL212. In the distal position of Q_B, the pK_a of GluL212 is estimated to be ≤6 while it is ∼10 in the proximal position (*73*−*75*). Therefore, a fraction of GluL212 in the ionized state would exist in a large pH range. Using a different approach−molecular dynamics simulations of Q_B binding in *Rb. sphaeroides* RCs−Grafton and Wheeler (*44*) have similarly attributed the differences in binding sites of Q_B to different protonation states of the GluL212/AspL213 cluster.

The Mulkidjanian model correlates with previously suggested mechanistic schemes of the Q_B turnover in *Rps. viridis* (*17*) and *Rb. sphaeroides* (*19*) RCs. It also provides an interesting way to reconcile proton uptake, electrogenic, and FTIR data taking into account two populations of GluL212, i.e., Glu-COO^- and Glu-COOH. In the AlaL212 mutant, the interaction between the methoxy oxygen O3 of Q_B and the side chain of Ala would not be possible. In the GlnL212 mutant, either no hydrogen bond is formed or Gln could still form a hydrogen bond to Q_B but no proton uptake would be necessary to form this hydrogen bond.[3] As a consequence, the pH-dependent curves of proton uptake (H^+/Q_B^-) of the GlnL212 and AlaL212 mutant RCs do not show the second maximum, i.e., the high-pH component (*34*). In native RCs at pH 7, protonation of GluL212 is coupled to the formation of Q_B^-. Accordingly, we propose that FTIR measurements on wild-type RCs monitor proton uptake by the fraction of ionized Glu L212 corresponding to RCs in which Q_B is bound in the distal site. Future FTIR work involving the detailed analysis of the pH dependence of the 1728 cm^{-1} band will be important to clarify GluL212 contribution to (global) proton uptake at high pH.

In conclusion, FTIR spectroscopy provides specific information compared to global proton uptake measurements since

[3] The importance of the conformation of the methoxy groups on the vibrational properties of ubiquinones has been inferred from experimental data on isotopically labeled quinones (*63*) and from quantum chemical calculations (*82*). However, in the absence of data on ubiquinone models with hydrogen bonding to one of the methoxy oxygen atoms, conclusions on the presence or absence of such a hydrogen bond to Q_B in native or mutant RCs cannot be drawn from the single observation of the FTIR bands at 1290 and 1265 cm^{-1}. These bands, which have been in part assigned to C−O−C vibrations from the methoxy groups (*63*) on the basis of studies of RCs reconstituted with ubiquinones labeled on the carbonyls, could even be insensitive to hydrogen bonding.

it monitors proton uptake by the carboxylic acid groups. The present data strengthen the structural and functional homologies nearby Q_B in the RCs of *Rb. capsulatus* and *Rb. sphaeroides*. It is thus probable that the structural organization of most of the side chains (and ordered water molecules) along the presumed proton-transfer pathways to Q_B is closely related in *Rb. sphaeroides* (*18*, *19*, *76*, *77*) and *Rb. capsulatus* RCs. In both RCs, the IR signature of a hydrogen-bond network has been found in the same spectral range. In both RCs, proton binding by the internal residue GluL212 occurs already at pH 7 upon the first electron transfer to Q_B, consistent with the Mulkidjanian model (*73*−*75*).

ACKNOWLEDGMENT

We thank Marianne Schiffer and Winfried Leibl for helpful discussions on hydrogen-bonding character and proton transfer.

REFERENCES

1. Feher, G., Allen, J. P., Okamura, M. Y., and Rees, D. C. (1989) *Nature 339*, 111−116.
2. Lavergne, J., Matthews, C., and Ginet, N. (1999) *Biochemistry 38*, 4542−4552.
3. Maróti, P., and Wraight, C. A. (1988) *Biochim. Biophys. Acta 934*, 329−347.
4. McPherson, P. H., Okamura, M. Y., and Feher, G. (1988) *Biochim. Biophys. Acta 934*, 348−368.
5. Miksovska, J., Schiffer, M., Hanson, D. K., and Sebban, P. (1999) *Proc. Natl. Acad. Sci. U.S.A. 96*, 14348−14353.
6. Gunner, M. R., and Honig, B. (1992) in *The Photosynthetic Bacterial Reaction Center II* (Breton, J., and Verméglio, A., Eds.) pp 403−410, Plenum Press, New York.
7. Beroza, P., Fredkin, D. R., Okamura, M. Y., and Feher, G. (1995) *Biophys. J. 68*, 2233−2250.
8. Lancaster, C. R. D., Michel, H., Honig, B., and Gunner, M. R. (1996) *Biophys. J. 70*, 2469−2492.
9. Rabenstein, B., Ullmann, G. M., and Knapp, E.-W. (1998) *Eur. Biophys. J. 27*, 626−637.
10. Alexov, E. G., and Gunner, M. R. (1999) *Biochemistry 38*, 8253−8270.
11. Alexov, E., Miksovska, J., Baciou, L., Schiffer, M., Hanson, D. K., Sebban, P., and Gunner, M. R. (2000) *Biochemistry 39*, *5940*−*5952*.
12. Allen, J. P., Feher, G., Yeates, T. O., Komiya, H., and Rees, D. C. (1988) *Proc. Natl. Acad. Sci. U.S.A. 85*, 8487−8491.
13. El-Kabbani, O., Chang, C.-H., Tiede, D., Norris, J., and Schiffer, M. (1991) *Biochemistry 30*, 5361−5369.
14. Ermler, U., Fritzsch, G., Buchanan, S. K., and Michel, H. (1994) *Structure 2*, 925−936.
15. Deisenhofer, J., and Michel, H. (1989) *EMBO J. 8*, 2149−2170.
16. Lancaster, C. R. D., Ermler, U., and Michel, H. (1995) in *Anoxygenic Photosynthetic Bacteria* (Blankenship, R. E., Madigan, M. T., and Bauer, C. E., Eds.) pp 503−525, Kluwer Academic Publishers, Dordrecht, The Netherlands.
17. Lancaster, C. R. D., and Michel, H. (1997) *Structure 5*, 1339−1359.
18. Abresch, E. C., Paddock, M. L., Stowell, M. H. B., McPhillips, T. M., Axelrod, H. L., Soltis, S. M., Rees, D. C., Okamura, M. Y., and Feher, G. (1998) *Photosynth. Res. 55*, 119−125.
19. Stowell, M. H. B., McPhillips, T. M., Rees, D. C., Soltis, S. M., Abresch, E., and Feher, G. (1997) *Science 276*, 812−816.
20. Fritzsch, G., Kampmann, L., Kapaun, G., and Michel, H. (1998) *Photosynth. Res. 55*, 1−6.
21. Takahashi, E., and Wraight, C. A. (1994) in *Advances in Molecular and Cell Biology: Molecular Processes in Photosynthesis* (Barber, J., Ed.) pp 197−251, JAI Press, Greenwich, CT.
22. Okamura, M. Y., and Feher, G. (1995) in *Anoxygenic Photosynthetic Bacteria* (Blankenship, R. E., Madigan, M. T., and Bauer, C. E., Eds.) pp 577−594, Kluwer Academic Publishers, Dordrecht, The Netherlands.
23. Sebban, P. Maróti, P., and Hanson, D. K. (1995) *Biochimie 77*, 677−694.
24. Paddock, M. L., McPherson, P. H., Feher, G., and Okamura, M. Y. (1990) *Proc. Natl. Acad. Sci. U.S.A. 87*, 6803−6807.
25. Paddock, M. L., Feher, G., and Okamura, M. Y. (1995) *Biochemistry 34*, 15742−15750.
26. Takahashi, E., and Wraight, C. A. (1990) *Biochim. Biophys. Acta 1020*, 107−111.
27. Paddock, M. L., Rongey, S. H., McPherson, P. H., Juth, A., Feher, G., and Okamura, M. Y. (1994) *Biochemistry 33*, 734−745.
28. Takahashi, E., and Wraight, C. A. (1992) *Biochemistry 31*, 855−866.
29. Hanson, D. K., Baciou, L., Tiede, D. M., Nance, S. L., Schiffer, M., and Sebban, P. (1992) *Biochim. Biophys. Acta 1102*, 260−265.
30. Hanson, D. K., Tiede, D. M., Nance, S. L., Chang, C.-H., and Schiffer, M. (1993) *Proc. Natl. Acad. Sci. U.S.A. 90*, 8929−8933.
31. Paddock, M. L., Rongey, S. H., Feher, G., and Okamura, M. Y. (1989) *Proc. Natl. Acad. Sci. U.S.A. 86*, 6602−6606.
32. McPherson, P., H., Schönfeld, M., Paddock, M. L., Okamura, M. Y., and Feher, G. (1994) *Biochemistry 33*, 1181−1193.
33. Hanson, D. K., Deng, Y.-L., Sebban, P., and Schiffer, M. (1995) *in Photosynthesis: from Light to Biosphere* (Mathis, P., Ed.), Vol. I, pp 859−862, Kluwer Academic Publishers, Dordrecht, The Netherlands.
34. Miksovska, J., Kálman, L., Schiffer, M., Maróti, P., Sebban, P. and Hanson, D. K. (1997) *Biochemistry 36*, 12216−12226.
35. Miksovska, J., Valério-Lepiniec, M., Schiffer, M., Hanson, D. K., and Sebban, P. (1998) *Biochemistry 37*, 2077−2083.
36. Hanson, D. K., Nance, S. L., and Schiffer, M. (1992) *Photosynth. Res. 32*, 147−143.
37. Maróti, P., Hanson, D. K., Baciou, L., Schiffer, M., and Sebban, P. (1994) *Proc. Natl. Acad. Sci. U.S.A. 91*, 5617−5621.
38. Sebban, P., Maróti, P., Schiffer, M., and Hanson, D. K. (1995) *Biochemistry 34*, 8390−8397.
39. Rongey, S. H., Paddock, M. L., Feher, G., and Okamura, M. Y. (1993) *Proc. Natl. Acad. Sci. U.S.A. 90*, 1325−1329.
40. Paddock, M. L., Senft, M. E., Graige, M. S., Rongey, S. H., Turanchik, T., Feher, G., and Okamura, M. Y. (1998) *Photosynth. Res. 55*, 281−291.
41. Valério-Lepiniec, M., Miksovska, J., Schiffer, M., Hanson, D. K., and Sebban, P. (1999) *Biochemistry 38*, 390−398.
42. Maróti, P., Hanson, D. K., Schiffer, M., and Sebban, P. (1995) *Nat. Struct. Biol. 2*, 1057−1059.
43. Brzezinski, P., Paddock, M. L., Okamura, M. Y., and Feher, G. (1997) *Biochim. Biophys. Acta 1321*, 149−156.
44. Grafton, A. K., and Wheeler, R. A. (1999) *J. Phys. Chem. 103*, 5380−5387.
45. Mäntele, W. (1993) *Trends Biochem. Sci. 18*, 197−202.
46. Siebert, F. (1993) in *Biomolecular Spectroscopy* (Clark, R. J. H., and Hester, R. E., Eds.) John Wiley & Sons: New York, Part A, pp 1−54.
47. Nabedryk, E., Breton, J., Hienerwadel, R., Fogel, C., Mäntele, W., Paddock, M. L., and Okamura, M. Y. (1995) *Biochemistry 34*, 14722−14732.
48. Hienerwadel, R., Grzybek, S., Fogel, C., Kreutz, W., Okamura, M., Y., Paddock, M. L., Breton, J., Nabedryk, E., and Mäntele, W. (1995) *Biochemistry 34*, 2832−2843.
49. Nabedryk, E., Breton, J., Okamura, M. Y., and Paddock, M. L. (1998) in *Photosynthesis: Mechanisms and Effects* (Garab, G., Ed.), Vol. II, pp 845−848, Kluwer Academic Publishers, Dordrecht, The Netherlands.
50. Nabedryk, E., Breton, J., Hienerwadel, R., Fogel, C., Mäntele, W., Paddock, M. L., and Okamura, M. Y. (1995) in *Photosynthesis: from Light to Biosphere* (Mathis, P., Ed.), Vol. I, pp 875−878, Kluwer Academic Publishers, Dordrecht, The Netherlands.

51. Nabedryk, E., Breton, J., Okamura, M. Y., and Paddock, M., L. (1998) *Biochemistry 37*, 14457−14462.
52. Youvan, D. C., Bylina, E., J., Alberti, M., Begusch, H., and Hearst, J. E. (1984) *Cell 37*, 949−957.
53. Williams, J. C., Steiner, L. A., and Feher, G. (1986) *Proteins: Struct., Funct., Genet. 1*, 312−325.
54. Komiya, H., Yeates, T. O., Rees, D. C., Allen, J. P., and Feher, G. (1988) *Proc. Natl. Acad. Sci. U.S.A. 85*, 9012−9016.
55. Schiffer, M., Chan, C.-K. Chang, C.-H., DiMagno, T. J., Fleming, G. R., Nance, S., Norris, J., Snyder, S., Thurnauer, M., Tiede, D. M., and Hanson D. K. (1992) in *The Photosynthetic Bacterial Reaction Center II* (Breton, J., and Verméglio, A., Eds.) pp 351−361, Plenum Press, New York.
56. Nabedryk, E., Breton, J., Joshi, H., and Hanson, D. K. (2000) *Biophys. J. 78*, 338A.
57. Miksovska, J., Maróti, P., Tandori, J., Schiffer, M., Hanson, D. K., and Sebban, P. (1996) *Biochemistry 35*, 15411−15417.
58. Goldsmith, J. O., and Boxer, S. G. (1996) *Biochim. Biophys. Acta 1276*, 171−175.
59. Nabedryk, E. (1999) *Biochim. Biophys. Acta 1411*, 206−213.
60. Breton, J., Thibodeau, D. L., Berthomieu, C., Mäntele, W., Verméglio, A., and Nabedryk, E. (1991) *FEBS Lett. 278*, 257−260.
61. Breton, J., Nabedryk, E., Allen, J. P., and Williams, J., C. (1997) *Biochemistry 36*, 4515−4525.
62. Breton, J., Berthomieu, C., Thibodeau, D. L., and Nabedryk, E. (1991) *FEBS Lett. 288*, 109−113.
63. Breton, J., Boullais, C., Berger, G., Mioskowski, C., and Nabedryk, E. (1995) *Biochemistry 34*, 11606−11616.
64. Brudler, R., de Groot, H. J. M., van Liemt, W. B. S., Gast, P., Hoff, A. J., Lugtenburg, J., and Gerwert, K. (1995) *FEBS Lett. 370*, 88−92.
65. Bauscher, M., Nabedryk, E., Bagley, K., Breton, J., and Mäntele, W. (1990) *FEBS Lett. 261*, 191−195.
66. Bauscher, M., and Mäntele, W. (1992) *J. Phys. Chem. 96*, 11101−11108.
67. Breton, J., Bibikova, M., Oesterhelt, D., and Nabedryk, E. (1999) *Biochemistry 38*, 11541−11552.
68. Nabedryk, E. (1996) in *Infrared Spectroscopy of Biomolecules* (Mantsch, H. H., and Chapman, D., Eds.) pp 39−81, Wiley-Liss, Inc., New York.
69. Nabedryk, E., Andrianabinintsoa, S., Dejonghe, D., and Breton, J. (1995) *Chem. Phys. 194*, 371−378.
70. Breton, J., Burie, J.-R., Berthomieu, C., Berger, G., and Nabedryk, E. (1994) *Biochemistry 33*, 4953−4965.
71. Breton, J., Boullais, C., Burie, J.-R., Nabedryk, E., and Mioskowski, C. (1994) *Biochemistry 33*, 14378−14386.
72. Brudler, R., de Groot, H. J. M., van Liemt, W. B. S., Steggerda, W. F., Esmeijer, R., Gast, P., Hoff, A. J., Lugtenburg, J., and Gerwert, K. (1994) *EMBO J. 13*, 5523−5530.
73. Gopta, O. A., Bloch, D. A., Cherepanov, D. A., and Mulkidjanian, A. Y. (1997) *FEBS Lett. 412*, 490−494.
74. Mulkidjanian, A. Y. (1999) *FEBS Lett. 463*, 199−204.
75. Cherepanov, D. A., Bibikov, S. I., Bibikova, M. V., Bloch, D. A., Drachev, L. A., Gopta, O. A., Oesterhelt, D., Semenov, A. Y., and Mulkidjanian, A. Y. (2000) *Biochim. Biophys. Acta 1459*, 10−34.
76. Paddock, M. L., Graige, M. S., Feher, G., and Okamura, M. Y. (1999) *Proc. Natl. Acad. Sci. U.S.A. 96*, 6183−6188.
77. Axelrod, H. L., Abresch, E. C., Paddock, M. L., Okamura, M. Y., and Feher, G. (2000) *Proc. Natl. Acad. Sci. U.S.A. 97*, 1542−1547.
78. Venyaminov, S. Yu., and Kalnin, N. N. (1990) *Biopolymers 30*, 1243−1257.
79. Breton, J., and Nabedryk, E. (1998) *Photosynth. Res. 55*, 301−307.
80. Zundel, G. (1992) *Trends Phys. Chem. 3*, 129−156.
81. Breton, J., Bibikova, M., Oesterhelt, D., and Nabedryk, E. (1998) in *Photosynthesis: Mechanisms and Effects* (Garab, G., Ed.), Vol. II, pp 687−692, Kluwer Academic Publishers, Dordrecht, The Netherlands.
82. Burie, J.-R., Boullais, C., Nonella, M., Mioskowski, C., Nabedryk, E., and Breton, J. (1997) *J. Phys. Chem. B 101*, 6607−6617.

BI0013795